Microwave-assisted modification of activated carbon with ammonia for efficient pyrene adsorption

Xinyu Ge[a], Zhansheng Wu[a,b*], Zhilin Wu[b], YujunYan[a], Giancarlo Cravotto[b*], Bang-Ce Ye[a]

[a]School of Chemistry and Chemical Engineering, Shihezi University, Shihezi 832003, P.R. China

[b]Dipartimento di Scienza e Tecnologia del Farmaco, University of Turin, Torino 10125, Italy

Corresponding author: Zhansheng Wu, Shihezi University, Shihezi 832003, P.R. China

Tel: 86993-2055015, Fax: 86993-2057270, E-mail address: wuzhans@126.com.

Abstract: With the aim to enhance the adsorption properties of polycyclic aromatic hydrocarbons (PAHs) from aqueous solutions, coal-based activated carbon (CAC) was modified with three different protocols: *i*) ammonia treatment (A-CAC), *ii*) microwave radiation (M-CAC) *iii*) and combined microwave radiation in the presence of ammonia (MA-CAC). The original CAC and all the modified samples were characterized by SEM, nitrogen adsorption-desorption, Boehm method, point of zero charge, FTIR and XPS. The surface area increased from 764.96 to 1293.78 m^2/g for CAC and MA-CAC, whereas the total groups containing oxygen decreased from 1.57 to 0.25 mmol/g. The pyrene adsorption capacity of all the modified samples was higher than CAC and the adsorption process for pyrene to the equilibrium needed only 40 min. Adsorption isotherm fitting revealed that pyrene adsorbed from the monolayer process on CAC to multilayer process on the modified samples. The adsorption kinetics of pyrene onto carbons was described using the pseudo-second-order kinetic model. The adsorption capacity of the CAC and modified samples had a good positive correlation with surface area, carboxyl groups, and lactones groups. The modified samples, especially MA-CAC, showed an enhanced adsorption of pyrene opening the way to a more general application as efficient adsorbent for PAHs contaminant.

Keywords: Coal-based activated carbon; microwaves; ammonia; modification; PAHs

1. Introduction

The toxicity of aromatic hydrocarbons, particularly polycyclic aromatic hydrocarbons (PAHs), is well known because of their mutagenicity and carcinogenicity [1-3]. Because of the high risk for human health even at low concentrations, the content of PAHs has strict regulations on drinking water. The PAHs removal with conventional physicochemical methods, such as flocculation, sedimentation or filtration is a difficult task because of their chemical persistence and semi-volatile nature [2]. For this reason a big effort has been paid to develop more efficient methods for removing PAHs using pyrene as a model from water environment.

Several techniques, such as bioremediation [4], photo-catalyst degradation [5], and adsorption [6–8] have been applied successfully for the minimization of PAHs in wastewater of domestic and/or industrial plants and soils. However, adsorption is one of the most economical and effective techniques for removing organic pollutants [3] and the most commonly used porous media for the removal of contaminants from aqueous solution is activated carbon (AC) [9]. AC with high surface area and developed pore structures are widely used in a variety of industries for applications that include the separation/purification of liquids and gases, removal of toxic substances as catalysts and catalyst support [10, 11]. Kong et al., [1] showed that PAHs removal by soybean stalk–based carbon was superior to that of commercial AC by adsorption method. Xiao et al., showed that pyrene adsorption using CAC is a comparatively fast and effective process [7]. The adsorption of PAHs onto AC from various media such as oil, gaseous phase and water has been reported. Yakout

et al., found that low-cost AC derived from agricultural wastes is very effective in adsorption of naphthalene, phenanthrene and pyrene from aqueous solution [12]. Ania et al., showed that chemically modified activated carbons with a higher non-polar character (i.e., low oxygen content) have proven to be more efficient for naphthalene adsorption [13]. However, some modification effects of CAC was not significant [7-8, 14-15], and ammonia modified CAC adsorb PAHs solution is report rarely. Shaarani showed that surface modification of the activated carbon using ammonia was shown to be able to increase its adsorption capacity for 2, 4-DCP [16]. So far, CAC modification by ammonia treatments under microwave irradiation and the effect on PAHs adsorption from aqueous solution, still remain an unexplored area. Therefore, considering enhance alkaline of CAC to modification with ammonia via microwave radiation is of great significance.

Based on the functional groups types of AC, the surface may have acidic, basic, and/or neutral characteristics [17]. In recent years, a big research effort was focused on new process for AC surface modification and characterization, in order to enhance the affinity to specific pollutants [18–20]. The higher surface basicity of AC can improve the affinity to pollutants [17]. Among procedures to achieve this goal, simple treatments by ammonia under microwave irradiation can be quite effective [18–21]. In addition, AC is known to be an excellent microwave absorber; dielectric heating can change texture and distribution of surface functional groups that affect surface chemistry [22]. Volumetric microwaves dissipation on carbon particles by dipole rotation and ionic conduction is extremely efficient [21]. Microwave radiation has been successfully applied for the

preparation [7], modification [8] and regeneration [14-15] processes of AC even at industrial scale [23]. Therefore, modified CAC with ammonia combined via microwave radiation owned research value and significance.

In the present study, CAC was modified by combining microwave radiation in the presence of ammonia. Surface properties of CAC sample before and after modification were characterized by means of scanning electron micrograph (SEM), nitrogen adsorption-desorption, Boehm method, oxygen-containing groups and basicity properties, point of zero charge (pH_{PZC}), FTIR and XPS. The kinetic and isotherms data of the adsorption process were then analyzed to study the adsorption of pyrene from aqueous solutions on the carbon samples. The mechanism of pyrene adsorption is discussed in relation to the pores structure and surface chemical properties of carbon materials. The results obtained from the experiments warrant the need for seeking better, faster, and more effective methods for the adsorption of PAHs from aqueous solutions.

2. Experimental

2.1. CAC sample

The raw material coal was purchased from Xinjiang Tebian Electric Apparatus Stock Co., Ltd, China. CAC was prepared using potassium hydroxide activation via microwave irradiation under N_2 atmosphere (MM823LA6-NS, Midea) with appropriate modification technology. The microwave oven with 2.45 GHz frequency was punched holes to insert the quartzose tube and equipped with power and time controller. The potassium hydroxide/coal (w/w) ratio was 1:1 (5 g : 5

g), microwave radiation 10 min under 700 W power. The resulting product were dried in air-drying oven at 110 °C for 4 h and marked as CAC. All chemicals and reagents used were analytical grade.

2.2. Modification of CAC

2.2.1. The modification of CAC by ammonia impregnation

An amount of 5.0 g of dried CAC was immersed in 50 mL of 10 wt% ammonia solution (analytical reagent grade) at 35 °C for 12 h. After this time the treated CAC was separated by filtration and then dried at 110 °C for 4 h. The ammonia treated CAC was stored in a desiccator. The obtained sample was labeled as A-CAC.

2.2.2. Microwave-assisted modification of CAC

A 3.0 g dried CAC was placed in a quartz tube inside the microwave reactor. The modification treatment was carried under microwave irradiation 8 min and microwave power 500 W with N_2 flow (150 mL/min). Then the reactants were cooled to room temperature in N_2 atmosphere and then dried at 110 °C for 4 h. The modified CAC was labeled as M-CAC.

2.2.3. Microwave-assisted modification of CAC using ammonia

A 1.5 g of dried A-CAC was placed in a quartz tube inside the microwave reactor. The modification treatment was carried with 8 min microwave irradiation under power 500 W and N_2 flow (150 mL/min). Then cooled down and the obtained sample was labeled as MA-CAC.

2.3. Elemental analysis

Elemental analysis of the CAC and the modified samples was performed using elemental

115 analyzer (VARIOEL III analyzer).

116 *2.4. Texture structure characterization*

117 Scanning Electron Microscopy with Energy Dispersive System (LEO 1430VP) was used to
118 observe the surface morphology of the carbon samples. The SEM enables the direct observation of
119 the changes in the surface microstructures of the carbons due to the modifications.

120 The Brunauer-Emmett-Teller (BET) surface area (S_{BET}) and the porosity of the activated
121 carbons were determined by the adsorption of N_2 at 77 K, using a Quantachrome Instruments
122 Quadrasorb SI. The system operates by measuring the quantity of nitrogen adsorbed onto or
123 desorbed from a solid sample at different P/P_0 pressures. The dried and weighed samples (0.1 g)
124 were outgassed at 300 °C for 3 h under vacuum.

125 *2.5. Boehm titration and pH_{PZC} value determination*

126 The amphoteric characteristics of carbon materials were determined by the amount of the
127 surface functional groups using the Boehm acid-base titration [24]. The specific method of titration
128 referred to references [15, 24]. The titration value was measured three times for each sample and
129 then the amounts of acidic/basic functional groups were calculated using the average of the three
130 titration data.

131 By definition, pH_{PZC} is the pH at which the net surface charge of an adsorbent is zero. The
132 pH_{PZC} values were determined referring to reference [15].

133 *2.6. Fourier transform infrared spectroscopy (FTIR)*

FTIR spectra of the carbons were taken with a PHI5700 ESCA FTIR system using KBr disks prepared by mixing 0.5% of finely ground carbon sample in KBr. Pellet made of pure KBr was used as a reference sample for background measurements. The spectra were recorded from 4000 to 400 cm^{-1} at a resolution of 4 cm^{-1}.

2.7. Adsorption of pyrene on the CAC and the modified samples

PAHs have low solubility in water, thus ethanol is used as a co-solvent (30% v/v) for the solubilization of pyrene from aqueous solution. A series of pyrene solution used in the isothermal and kinetic experiments were prepared through diluting the stock solution with distill water.

2.8.1. Adsorption kinetic studies

For the adsorption kinetics experiments, pyrene adsorption was conducted in conical flasks at 20 °C. The initial concentration was set as 30 mg/L, and the carbon materials were taken out at different contacting time intervals (2-180 min). The whole mixture was separated by filtration, and pyrene concentration was measured using a UV-75N spectrophotometer at 237 nm. The amount of pyrene at time t, q_t (mg/g), was calculated by the following equation:

$$q_t = \frac{(C_0 - C_t) \times V}{m} \quad (1)$$

where q_t (mg/g) is amount of pollutant adsorbed per g of sorbent at time t (min). C_0 (mg/L) and C_t(mg/L) are the initial and residual concentration of pyrene solution, respectively. V (mL) is the volume of the aqueous solution, m (g/mol) is the molar mass of the carbons.

2.8.2. Adsorption isotherms studies

In the adsorption isotherms experiments, a 60 mg of the CAC or modified samples was added to 100 mL and 20-100 mg/L of pyrene solution, and then was contacted for 60 min at 60 rpm in a rotary mechanical shaker to reach equilibrium. The amount of pyrene adsorbed on the CAC and the modified samples at equilibrium, q_e (mg/g), can be calculated according to Eq. (2),

$$q_e = \frac{(C_0 - C_e) \times V}{m} \quad (2)$$

where q_e (mg/g) is the amount of adsorption of pyrene at equilibrium. C_0 and C_e (mg/L) are the initial and equilibrium concentrations of pyrene solution, respectively.

2.9 Regeneration of spent carbon

In this study, we choose the typical sample of MA-CAC to study the regeneration capacity. The MA-CAC sample adsorbed pyrene was desorbed and immersed in 100 mL ethanol for 90 min. The MA-CAC sample was removed and dried in vacuum at 110 °C. The regeneration of the MA-CAC sample was determined, and the pyrene adsorption capacity was calculated repeatedly. Desorption experiments were conducted again using the same adsorption method.

3. Results and discussion

3.1. Characterization method

3.1.1. Elemental analysis

Modification treatments produced major changes in the contents of carbon and oxygen (Table 1). In particular, the nitrogen content is always increased. In the MA-CAC sample surface, the content of nitrogen is 2.54%. The carbon content of the MA-CAC sample increased compared with

the CAC, while the content oxygen of the CAC decreased, which led to the ratio of C/O increase from 2.89 to 6.28. The change in major element can be explained with the following reason. Ammonia treatment can introduce nitrogen element into AC structure [19, 20]. In addition, Liu et al., [19] reported that modification of bamboo-based AC using microwave radiation, the acidic groups were decomposed and removed in the form of CO or CO_2, which led to the decreased of oxygen element. Thus, through microwave radiation using ammonia for modify the CAC obtained good basic properties. And XPS analysis had the same element analysis results referring to Table S1 in the Supplementary Data.

Table 1 should be put here.

3.1.2. Observation by SEM

As shown in Fig. 1(a), the SEM micrograph of the CAC has some pore structures and attached fine particles over its surface, which formed a system of complicated pore networks. The surfaces of A-CAC, M-CAC, and MA-CAC in Figs. 1(b-d) were highly porous, which could enhance specific surface area for improving adsorption of PAHs from aqueous solution. The morphologies usually have important functions in the adsorption procedure [25]. The SEM images of the modified samples show large pores. We can see that the pore texture of the CAC changed after the modification treatment, and the three carbons still keep a rich pore structure. The MA-CAC samples have a well-developed pore structure, and these pores were arranged neatly and uniformly.

Fig. 1 should be put here.

191 *3.1.3. BET analysis*

192 According to IUPAC classification, the nitrogen adsorption isotherms of the CAC and the
193 modified samples are essentially of type IV with a type-H_4 hysteresis loop (Fig. 2). However, the
194 CAC and the modified samples showed the same type of hysteresis. This characteristic indicates
195 that absorbents present a mesoporous structure. Song et al. found that each isotherm showed a
196 distinct hysteresis loop, which is associated with the capillary condensation in mesopores, and thus
197 carbon is characteristic of mesoporous adsorbents [26].

198 For the carbon samples, most pores have diameters of small mesopores with approximately 2-4
199 nm. Moreover, the average pore size is increased from 3.111 nm to 3.831 nm for the CAC and
200 MA-CAC, which is mainly because of the transition of micropores into mesopores after a highly
201 corrosive modification process [27]. However, the average pore sizes for the M-CAC and the
202 MA-CAC only increase from 3.830 nm to 3.831 nm, which a little increase from the M-CAC to the
203 MA-CAC. Detailed information regarding the textural properties of the CAC and modified samples
204 is presented in Fig. 3. The modification enhances pore volume and surface area of the adsorbents.
205 The BET surface area of samples is increased from 764.96 to 1293.78 m^2/g, i.e., from CAC to
206 MA-CAC. Compared to those of the untreated CAC sample, the total pore volume of A-CAC,
207 M-CAC and MA-CAC increase approximately 5.70%, 45.00% and 102.04%, respectively (Fig. 3).
208 These results suggested that modified samples are generally conducive to a well-developed pore
209 structure of activated carbons. As mentioned in our previous study, the specific surface area and

pore structure of the CAC are important in determining the adsorption of PAHs performance using the modified samples under microwave radiation [15]. The adsorption capacity of PAHs (Pyrene) is also expected to increase because the specific surface area and pore volume of the CAC increased for different modified treatments. Compared with the CAC and the modified samples, the considerable changes of the surface area and average pore size on the M-CAC and MA-CAC samples should be attributed to the distinct mechanism of microwave radiation. As a result, the interior part of M-CAC and MA-CAC are heated more favorably under microwave radiation, which facilitates the modification process [19].

Fig. 2 should be put here.

Fig. 3 should be put here.

3.1.4. Boehm titration, surface acidity, and basicity and pH_{PZC} value

To confirm how the different modification treatments alter the chemistry characteristics of the CAC, the content of surface functional groups on the carbon samples as well as their points of zero charge (pH_{PZC}) have been ascertained. The surface acidity, basicity and functional groups of CAC and the modified samples are listed in Fig. 4. The total acidic groups on the modified CAC are obviously less than those on the CAC. Carboxyl, lactone, and phenol groups all decreased after modification treatment. Moreover, the total acidic groups in the modified samples decrease as the following order: MA-CAC < M-CAC < A-CAC < CAC. Simultaneously, the number of basic groups of all modified samples increase significantly than that of the CAC sample, as expected. The

basic groups of the MA-CAC are the most and approximately twice the value obtained for the CAC. For the decrease of acidic groups in the microwave treatment sample, which can be explained by decomposed and removed in the form of CO or CO_2 under microwave radiation [28]. Przepiorski et al., study high temperature ammonia treatment of AC and indicated that nitrogen is introduced into structure of AC according to treatment with ammonia [29], thus the MA-CAC and A-CAC exhibit the higher basicity. These results are consistent with the XPS survey spectra of CAC and the modified samples referring to the Supplementary Data in Fig. S1. The content of oxygen element decreased into the modified samples surface. Therefore, we can conclude that the modification with ammonia via microwave radiation can increase the basicity effectively, as well as remove oxygen-containing groups.

The pH_{PZC} increases from 6.83 of the CAC to 12.23 of the MA-CAC (Fig. 4), which is in accordance with the results of the acid-base titration results. It is due to the decrease in acidity and increase in basicity made an increase in pH_{PZC} value after modification. This also implies that the three modification samples performed better basicity properties. Compared with the three modified samples, we believe that the modification method by ammonia using microwave radiation probably benefits for the obtained the highly-efficiency material for adsorption of PAHs from aqueous solution. In addition, impact of ionic strength on the adsorption of pyrene referred to Fig. S2, which showed in the supplementary materials.

Fig. 4 should be put here.

3.1.5. FTIR studies

The spectra are similar in all cases, which suggested that the CAC and the modified samples have similar structures and functional groups (Fig. 5). Firstly, the broad band at approximately 3450 cm^{-1}, which may be due to the O–H stretching vibration of hydroxyl functional groups including hydrogen bonding. The intense band at approximately 2920 cm^{-1} is attributed to the C–H stretching vibration, which decreased greatly for the modified CAC, indicating that the hydrogen element is removed to a large extent after modification by microwave radiation [19]. The result is consistent with the above elements analysis (Table 1). A band centered near 2300 cm^{-1} can be seen in the FTIR of all samples, the bands had been proposed to C-O bonds, which may be because of ketene. The band in the MA-CAC sample decreased significantly compared with that of CAC. Some bands in the range of 1600 cm^{-1} are left for the activated carbons, which were probably corresponded to the C=O stretching vibration. Another band was found at approximately 800 cm^{-1}, which is expected to be associated with the out-of-plane bending mode of O–H. The decrease of phenolic explained the decrease peak for the modified samples. The band centered at 470 cm^{-1} is attributed to C-N-C stretching model. The minimal acidic oxygen functional groups such as phenol and carboxyl groups of the modified sample may enhance the adsorption capacity of pyrene from aqueous solutions, as shown in the results of Boehm titration.

Fig. 5 should be put here.

3.2. Adsorption studies

3.2.1. Kinetics of pyrene on the CAC and modified samples

The kinetics of adsorption describes the rate of adsorbate adsorption on the CAC and modified samples and it controls the equilibrium time. The kinetic models of pseudo-first-order (Eq. (3)), pseudo-second-order (Eq. (4)), were applied to study the kinetics of the adsorption process, whereas the intraparticle diffusion model (Eq. (5)) was further tested to determine the diffusion mechanism of the adsorption system.

The pseudo-first-order kinetic rate equation is expressed as:

$$\frac{1}{q_t} = \frac{1}{q_e} + \frac{k_1}{q_e t} \quad (3)$$

where k_1 is the rate constant of pseudo-first-order sorption (min^{-1}).

The pseudo-second-order kinetic rate equation is expressed as:

$$\frac{t}{q_t} = \frac{1}{k_2 q_e^2} + \frac{t}{q_e} \quad (4)$$

where k_2 is the rate constant of pseudo-second-order sorption [g/(mg·min)].

In the intraparticle diffusion model, the relationship between the adsorption capacity at time t, q_t and $t^{0.5}$ could be written as:

$$q_t = K_p t^{0.5} + C \quad (5)$$

where K_p is the intraparticle diffusion constant [mg/(g·min)] and C is the intercept of the line, which is proportional to the boundary layer thickness.

In film diffusion model can be identified according to the following equation:

$$-\ln\left(1-\frac{q_t}{q_e}\right) = K_{bf}\, t \quad (6)$$

where K_{bf} is the liquid film diffusion constant (min^{-1}).

In Fig. 6, adsorption of pyrene on the carbon materials appear to have similar kinetic behaviors. The removal curves are single, smooth, and continuous. After 40 min of contact between the adsorbents and pyrene, the adsorption process tends to reach the equilibrium state. However, the time required for pyrene solution to reach equilibrium need more time in previous studies [2, 12, 30]. Yakout et al., reported that 100 mg of low-cost AC adsorb 100 mg/L of naphthalene, phenanthrene and pyrene in 20 mL solution required 24 h to adsorption equilibrium [12]. A 2 mg of modified periodic mesoporous organosilica (PMO) adsorption of PAHs aqueous solutions (8 mg/L, 5 mL) adsorption equilibrium also needed 24 h [2]. These studies suggested that the modified carbons in this work had the excellent adsorption performance compared with the works of previous research. From the kinetic curves in Fig. 6, we could draw a conclusion: the pyrene amounts adsorbed on the adsorbents had the following order: MA-CAC > M-CAC > A-CAC> CAC. The modified samples could adsorb efficiently and rapidly pyrene from aqueous.

Table 2 shows three kinetic models parameters obtained. When the higher R^2 value was considered simultaneously as indicative of the best fittings (Table 2), it was found that the pseudo-two-order model could best represented the kinetic data for pyrene adsorption with high correlation coefficient ($R^2 > 0.999$). In addition, pseudo-two-order model predicted the q_{exp} values closer to the experimental q_{cal} values than pseudo-first-order, which suggested that it was appropriate for describing pyrene adsorption on the carbons at equilibrium state. According to some

researchers, the pseudo-second-order model may be related to the occurrence of chemical sorption, which may control the reaction rate [31]. In addition, intraparticle diffusion kinetic models owned low-correlation coefficients ($0.2980 < R^2 < 0.6600$). In this study, the q_t versus $t^{0.5}$ graph is only initially linear which indicates that intraparticle diffusion could be involved in the sorption process of pyrene on both the CAC and modified samples. While this line not passes through the origin, intraparticle diffusion was not rate determining step [32]. Likewise, by comparing the data presented in Table 3, the R^2 values ($0.8420 < R^2 < 0.9540$) for the film diffusion model were higher than those of intraparticle diffusion model, thus suggesting that film diffusion could control the adsorption rate of pyrene onto carbons under the studied conditions [31].

If intraparticle diffusion is involved in the sorption process, a plot of the square root of time versus adsorption would result in a linear relationship, and the particle diffusion would be the determining step if this line passes through the origin.

Fig. 6 should be put here.

Table 3 should be put here.

3.2.2. Isotherms of pyrene on the CAC and modified samples

In order to optimize the adsorption process and to forecast adsorption, Langmuir and Freundlich isotherm models were applied to the equilibrium data. Langmuir model is based on the assumption of a homogeneous adsorbent surface, which can be written as:

$$\frac{C_e}{q_e} = \frac{1}{q_m} C_e + \frac{1}{q_m K_L} \quad (7)$$

where q_m (mg/g) is the maximal adsorption capacity, K_L(L/mg) is a constant related to the free energy of the adsorption.

Freundlich model is an empirical equation assuming heterogeneous adsorbent surface, which can be written as:

$$\ln q_e = \frac{1}{n} \ln C_e + \ln K_F \quad (8)$$

where K_F is the unit capacity factor related to the adsorbent capacity and n is an empirical parameter representing the heterogeneity of site energies, respectively.

The similar shapes of the isotherms for pyrene adsorption on CAC and the modified samples suggest that the adsorption process occurred via the similar pathways (Fig. 7). The modified samples for pyrene adsorption belong to the L type according to the Giles classification [15]. As shown in Fig. 7, the initial isotherms rise rapidly during the initial stage of adsorption when C_e and q_e values are both lower, there are many readily accessible sites available on the surface of carbons. However, the adsorption isotherms rate of decrease gradually at high concentrations, it is due to more time is required to reach to equilibrium. This is because that it is difficult for the molecules to penetrate the adsorbed layer of absorbent, which are filled as more sites [12]. For the CAC, the monolayer adsorption capacity of pyrene was 142.86 mg/g. And as presented in Fig. 7, all the modified samples have better adsorption properties for pyrene solution. The parameters of the two isotherm models are calculated and summarized in Table 3. In this work, the Langmuir isotherm best fits the experimental data of CAC samples for the adsorption of pyrene, indicating that the

adsorption process is a monolayer phenomenon [2, 8]. However, the Freundlich model have higher R^2 value ($R^2 \geqslant 0.9991$) for the modified samples. Therefore, the adsorption belongs to a multilayer process, which means that the modification treatments probably make the adsorption of pyrene became multilayer adsorption and adsorption more effectively. Moreover, all 1/n values between 0.1 and 1.0 indicate a strong interaction between adsorbent and pyrene with a favorable adsorption [2]. The results show that the equilibrium adsorption data fitted well with the Freundlich model, which could adequately describe the adsorption behavior of pyrene onto the modified samples.

The pyrene adsorption from wastewaters on different adsorbents such as PMO, chitin, green coconut shell, and immature coal [2, 30, 33] had been investigated. The intensity of adsorption and the Freundlich adsorption constant K_F calculated for each adsorption system are given in Table 4. A comparison between the CAC and the modified samples indicate that the modified samples in our study have a good and effective adsorption for pyrene from aqueous solution.

Fig. 7 should be put here.

Table 3 should be put here.

Table 4 should be put here.

3.2.3. Thermodynamic parameters

Thermodynamic parameters were evaluated to confirm the adsorption nature of CAC and MCAC. The thermodynamic constants, free energy change (ΔG^o, kJ/mol), enthalpy change (ΔH^o, kJ/mol) and entropy change (ΔS^o, J/(K·mol)) were calculated. The thermodynamics equations were

as following:

$$\Delta G^{o} = -RT \ln K_F \quad (10)$$

$$\Delta G^{o} = \Delta H^{o} - T\Delta S^{o} \quad (11)$$

$$\ln K_F = \frac{\Delta S^{\theta}}{R} - \frac{\Delta H^{\theta}}{RT} \quad (12)$$

where K_F is the adsorption equilibrium constant in Eq. (8) for pyrene.

The ΔG^{o} values of the different carbons for pyrene adsorption were decreased with an increase in temperature (Table 5). This indicates that the adsorption process was spontaneous and the spontaneity decreased with the temperature increasing. This shows that the removal process is favored at lower temperature; it was consistent with the results obtained in our previous study [7]. The negative value of ΔH^{o} indicated an exothermal adsorption process, which indicated the removal process for pyrene was generally favored at a low temperature. It was in agreement with what described above. The positive values ΔS^{o} obtained shows the affinity of carbon materials for pyrene and the increasing randomness at the solid-solution interface during the adsorption process [15, 34].

Table 5 should be put here.

3.3. The effect of surface physicochemical characteristics on adsorption capacity

The adsorption capacity of AC rely on their surface characteristics, e.g. texture and surface physicochemical properties [35]. Comparing the relationship of the adsorption capacity of PAHs and their surface characteristics is necessary. This comparison will provide a good basis for better orientation of the modified CAC. Correlation analysis is used for studying the effects of some

381 factors on pyrene adsorption, which is shown in Figs. 8(a–c). The BET surface area presents a
382 certain correlation with the adsorption capacity of pyrene for the CAC and the modified samples
383 (Fig. 8). This BET surface area suggests that a high surface area would generally result in a high
384 adsorption capacity for pyrene solution. For the all samples, MA-CAC has the highest BET surface
385 area (Fig. 8), thus it implies the highest adsorption capacity of pyrene solution. In addition,
386 MA-CAC has the largest pore volume than other carbons in this work. However, the other modified
387 samples (A-CAC and M-CAC) had a similar result, i.e., they have a higher pyrene adsorption than
388 the CAC. Fig. 8 shows that the adsorption capacities of the CAC and modified carbons increased
389 with the decrease in total surface oxygen-containing groups. The MA-CAC containing the least
390 surface oxygen groups present the highest adsorption capacities for pyrene. From Fig. 8b we can
391 see that the amount of surface oxygen containing groups, especially carboxylic functional and
392 lactones groups, have good linear correlations with R^2=0.945 and R^2=0.987. This result could be
393 explained using the low surface oxygen that is beneficial to the adsorption of pyrene solution. The
394 result is similar to that of previous reports [36].

395 Moreover, the basicity properties and adsorption of pyrene have a linear correlation (R^2=0.857).
396 Higher basicity can increase the affinity of the modified samples to pyrene, and consequently the
397 modified samples sites are more available for the PAHs molecules. The enhanced basicity may
398 attribute to $–NH_2$ and nitrogen-containing groups introducing into the MA-CAC surface (Fig. 9). In
399 addition, combined microwave radiation in the presence of ammonia modification increases the

amount of nitrogen atoms (2.54%) on MA-CAC surface (Table 1). Thus it increases the affinity of the alkaline MA-CAC samples to pyrene solution [17]. This could be explained by the fact that PAHs and benzene molecules from π-π complex and enhanced the interaction between the π-electrons of benzene rings and active sites on the MA-CAC sample surface [37, 38].

In all, basicity, carboxylic functional and lactones higher affect the adsorption of pyrene. In our previous study, the adsorption pyrene on CAC or A-CACs modified by different ammonia concentrations had the similar results that the higher basicity and lower acidity is beneficial to pyrene adsorption. The high surface area, the amount of low oxygen-containing groups and basicity of the modified samples made them good adsorption properties for pyrene from aqueous solution.

Fig. 8 should be put here.

Fig. 9 should be put here.

3.4 Regeneration of the MA-CAC sample

The MA-CAC sample still had a high adsorption capacity for pyrene, which reached a level of 90.30% of the initial value after three cycles (Fig. 10). This indicated that the MA-CAC samples had good stability, reusability, and effective adsorption for pyrene from aqueous solutions.

Fig. 10 should be put here.

4. Conclusions

With the aim to enhance PAHs adsorption from aqueous solution, different procedures of CAC modification have been compared: *i)* with ammonia, *ii)* with microwave radiation and *iii)* with

ammonia under microwave. This study showed that all modified samples had higher adsorption capacity for pyrene than the CAC, especially the MA-CAC sample. It is attributed to the significant decrease of the oxygen-containing functional groups of MA-CAC. Meanwhile, BET surface area, total pore volume and average pore size were increased most distinct, compared with the CAC.

The kinetics of pyrene with the CAC and the modified samples showed a similar behavior. After 40 min of contact between the adsorbent and pyrene, a tendency of the system to reach the equilibrium was observed, and MA-CAC showed the highest adsorption capacity with 61.96 mg/g. The adsorption isotherm experimental data were best described using the Freundlich isotherm model for the modified samples, and the kinetic model of pseudo-second order best represented the adsorption kinetic data of pyrene for the CAC and the modified samples. Thus, pyrene adsorbs on the modified samples from the monolayer process to multilayer process. Moreover, we can conclude that the adsorption of pyrene is a chemical sorption, which may control the reaction rate. The sorption of pyrene onto carbons was spontaneous, exothermal, and entropically driven. The modified CAC has a great potential as absorbents for the adsorption of PAHs from aqueous solution and the adsorption process is fast and effective. We concluded that obtaining a high surface area, low oxygen-containing groups, and a high basicity are necessary to improve the activated carbons for pyrene adsorption capacity. The MA-CAC sample from the microwave-assisted treatment with ammonia is a low cost, high adsorption capacity, and regeneration efficiency adsorbent with great potential industrial applications.

Acknowledgments

This work was supported financially by funding from the National Natural Science Foundation of China (51262025) and International scientific and technological cooperation project of Xinjiang Bingtuan (2013BC002).

References

[1] H.L. Kong, J. He, Y.Z. Gao, J. Han, X.Z. Zhu, J. Environ. Qual. 40 (2011) 1-8.

[2] C.B. Vidal, A.L. Barros, C.P. Moura, A.C.A. de Lima, F.S. Dias, L.C.G. Vasconcellos, P.B.A. Fechine, R.F. Nascimento, J. Colloid Interf. Sci. 357 (2011) 466-473.

[3] M.J. Yuan, S.T. Tong, S.Q. Zhao, C.Q. Jia, J. Hazard. Mater. 181 (2010) 1115-1120.

[4] B.V. Chang, S.W. Chang, S.Y. Yan, Adv. Environ. Res. 7 (2003) 623-628.

[5] Seul-Yi Lee, Soo-Jin Park, J. Ind. Eng. Chem. 19(2013) 1761-1769.

[6] A.M. Ghaedi, M. Ghaedi , A. Vafaei, N. Iravani, M. Keshavarz, M. Rad, I. Tyagi, S. Agarwalc, V. K. Gupta, J. Mol. Liq. 206 (2015): 195-206.

[7] X.M. Xiao, F. Tian, Y.J. Yan, Z.S. Wu, J. Shihezi Univ. 32 (2014) 485-490.

[8] X.Y. Ge, Z.S. Wu, Y.J. Yan, Y.X. Zeng, J. Shihezi Univ. 34 (2016): 92-99.

[9] B.L. Chen, M.X. Yuan, H. Liu, J. Hazard. Mater. 188 (2011) 436-442.

[10] K.B Yang, J.H. Peng, C. Srinivasakannan, L.B. Zhang, H.Y. Xia, X.H. Duan, Bioresource Technol. 101 (2010) 6163-6169.

[11] S.H. Moon, J.W. Shim, J. Colloid Interf. Sci. 298 (2006) 523-528.

[12] S. M. Yakout, A. A. M. Daifullah, S. A. El-Reefy, Adsorpt. Sci. Technol. 31 (2013) 293-302.

[13] C.O. Ania, B. Cabal, C. Pevida, A. Arenillas, J.B. Parra, F. Rubiera, J.J. Pis, Water Res. 41

(2007) 333-340.

[14] V.K. Gupta, I. Tyagi, S. Agarwal, O. Moradi, H. Sadegh, R. Shahryari-ghoshekandi, A.S.H. Makhlouf, M. Goodarzi, A. Garshasbi, Crit. Rev. Env. Sci. Tec. 42(2016): 93-118.

[15] X.Y. Ge, F. Tian, Z.L. Wu, Y.J. Yan, G. Cravotto, Z.S. Wu, Chem. Eng. Process. 91 (2015) 67-77.

[16] F.W. Shaarani, B.H. Hameed, Chem. Eng. J. 169 (2011) 180-185.

[17] V.K. Gupta, A. Nayak, S. Agarwal, I. Tyagi, J. Colloid Interf. Sci., 417 (2014) 420-430.

[18] Z.J. Zhang, M.Y. Xu, H.H. Wang, Z. Li, Chem. Eng. J. 160 (2010) 571-577.

[19] Q.S. Liu, T. Zheng, N. Li, P. Wang, G. Abulikemu, Appl. Surf. Sci. 256 (2010) 3309-3315.

[20] S. Bashkova, T.J. Bandosz, J. Colloid Interf. Sci. 333 (2009) 97-103.

[21] L.Q. Zhang, M. Mi, B. Li, Y. Dong, Res. J. Appl. Sci. Eng. Technol. 5 (2013) 1791-1795.

[22] R. Cherbanski, M. Komorowska-Durka, G.D. Stefanidis, A.I. Stankiewicz, Ind. Eng. Chem. Res. 50 (2011) 8632-8644.

[23] B. Heibati, S. Rodriguez-Couto, M.A. Al-Ghouti, M. Asif, I. Tyagi, S. Agarwal, V.K. Gupta, J. Mol. Liq. 208 (2015) 99–105.

[24] X.L. Song, H.Y. Liu, L. Cheng, Y.X. Qu, Desalination 255 (2010) 78-83.

[25] G.X. Yu, M. Jin, J. Sun, X.L. Zhou, L.F. Chen, J.A. Wang, Catal. Today 212 (2013) 31-37.

[26] L. Song, M. Junichi, K. Hirofumi, Carbon 44 (2006) 1884-1890.

[27] Jr.V. Strelko, D.J. Malik, J. Colloid Interf. Sci. 250 (2002) 213-220.

[28] C. Moreno-Castilla, F. Carrasco-Marin, A. Mueden, Carbon 35 (1997) 1619-1626.

[29] J. Przepiorski, M. Skrodzewicz, A.W. Morawski, Appl. Surf. Sci. 225 (2004) 235-242.

[30] Z.C. Zeledon-Toruno, C. Lao-Luque, F.X.C. de las Heras, M. Sole-Sardans, Chemosphere 67 (2007) 505-512.

[31] A. Benhouria, M.A. Islam, H. Zaghouane-Boudiaf, M. Boutahala, B.H. Hameed, Chem. Eng. J. 270 (2015) 621-630.

[32] C. Valderrama, X. Gamisans, X. de las Heras, A. Farran, J.L. Cortina, J. Hazard. Mater. 157 (2008) 386-396.

[33] R. Crisafulli, M.A.L. Milhome, R.M. Cavalcante, E.R. Silveira, D. Keukeleire, R.F. Nascimento, Bioresource Technol. 99 (2008) 4515-4519.

[34] S. Agarwal, I. Tyagi, V.K. Gupta , N. Ghasemi, M. Shahivand, M. Ghasemi, J. Mol. Liq. 218 (2016) 208-218.

[35] L. Li, S.Q. Liu, J.X. Liu, J. Hazard. Mater. 192 (2011) 683-690.

[36] T. Garcia, R. Murillo, D. Cazorla-Amoros, A.M. Mastral, A. Linares-Solano, Carbon 42 (2004) 1683-1689.

[37] A.M. Dowaidar, M.S. EI-Shahawi, I. Ashour, Sep. Sci. Technol. 42 (2007) 3609-3622.

[38] X.M. Xiao, D.D. Liu, Y.Y. Yana, Z.L. Wu, Z.S. Wu, G. Cravotto, J. Taiwan Inst. Chem. Eng. 53 (2015) 160-167.

[39] S. Dağdelen, B. Acemioğlu, E. Baran, O. Koçer, Water Air Soil Pollut. 225 (2014) 1899-1914.

508 **Fig. 1.** Scanning electron micrographs of CAC and the modified samples (a) CAC; (b) A-CAC; (c)

509 M-CAC; (d) MA-CAC

510 **Fig. 2.** Nitrogen adsorption-desorption isotherms and pores size distribution of different activated

511 carbons: (a) CAC; (b) A-CAC; (c) M-CAC; (d) MA-CAC

512 **Fig. 3.** Comparison of BET surface area and the porous texture of the CAC and the modified

513 samples (a) BET surface area; (b) Total pore volume

514 **Fig. 4.** The surface acidity, basicity, surface functional groups, and pH_{PZC} value of the CAC and the

515 modified samples

516 **Fig. 5.** FTIR spectra of the CAC and the modified samples

517 **Fig. 6.** Adsorbed amount of various carbon materials for pyrene as a function of adsorption time at

518 20 °C (pyrene concentration: 30 mg/L, pyrene solution volume: 100 mL, adsorbents amount: 60

519 mg)

520 **Fig. 7.** The adsorbed amount per gram of carbon materials for pyrene as a function of pyrene

521 concentration in solutions at 20 °C (pyrene solution volume: 100 mL, adsorbents amount: 60 mg)

522 **Fig. 8.** Adsorption capacity of CAC and the modified samples for pyrene as a function of BET

523 surface area (a); Oxygen-containing groups (b); Basic groups (c)

524 **Fig . 9.** The change in functional groups of CAC modified to MA-CAC

525 **Fig. 10.** Adsorption capacities of pyrene onto MA-CAC for three cycles

526

527

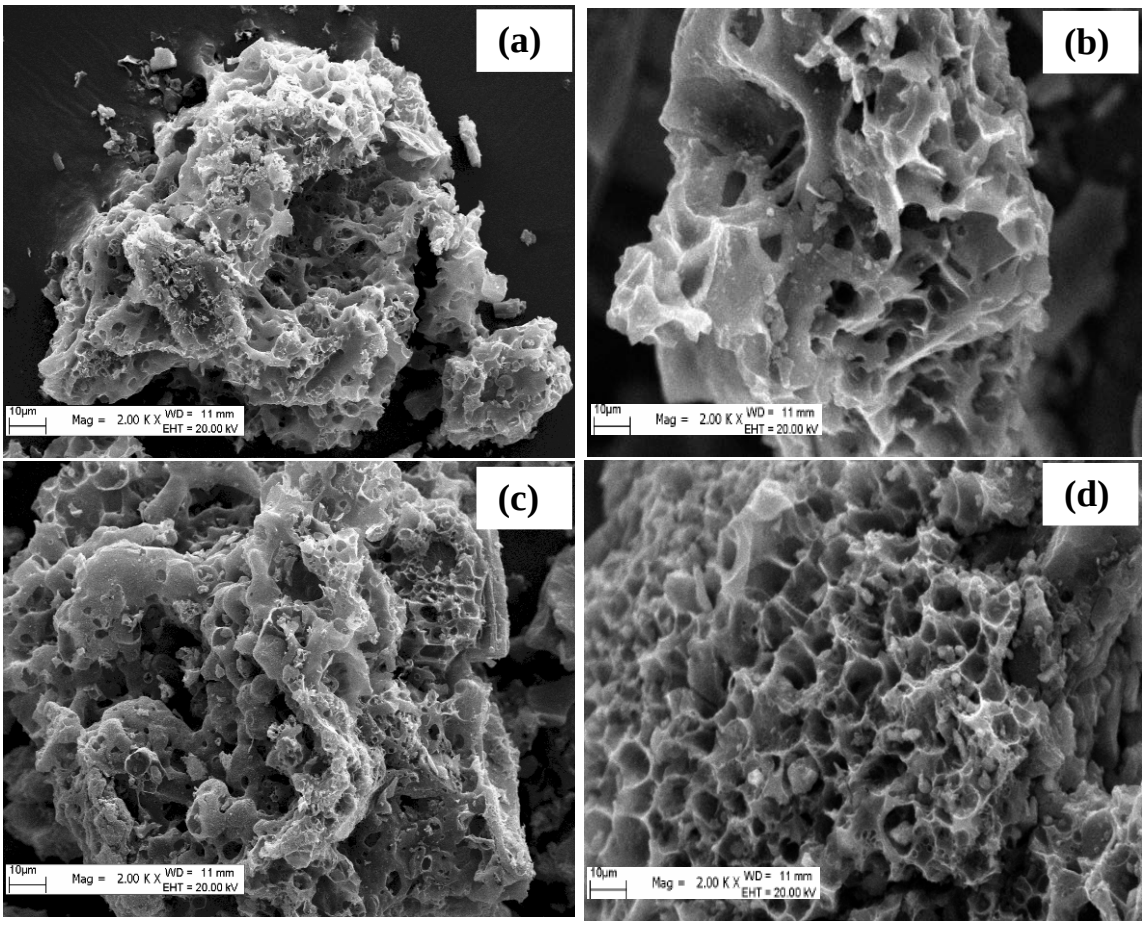

528 **Fig. 1.** Scanning electron micrographs of CAC and the modified samples (a) CAC; (b) A-CAC; (c)

529 M-CAC; (d) MA-CAC

530

531

532

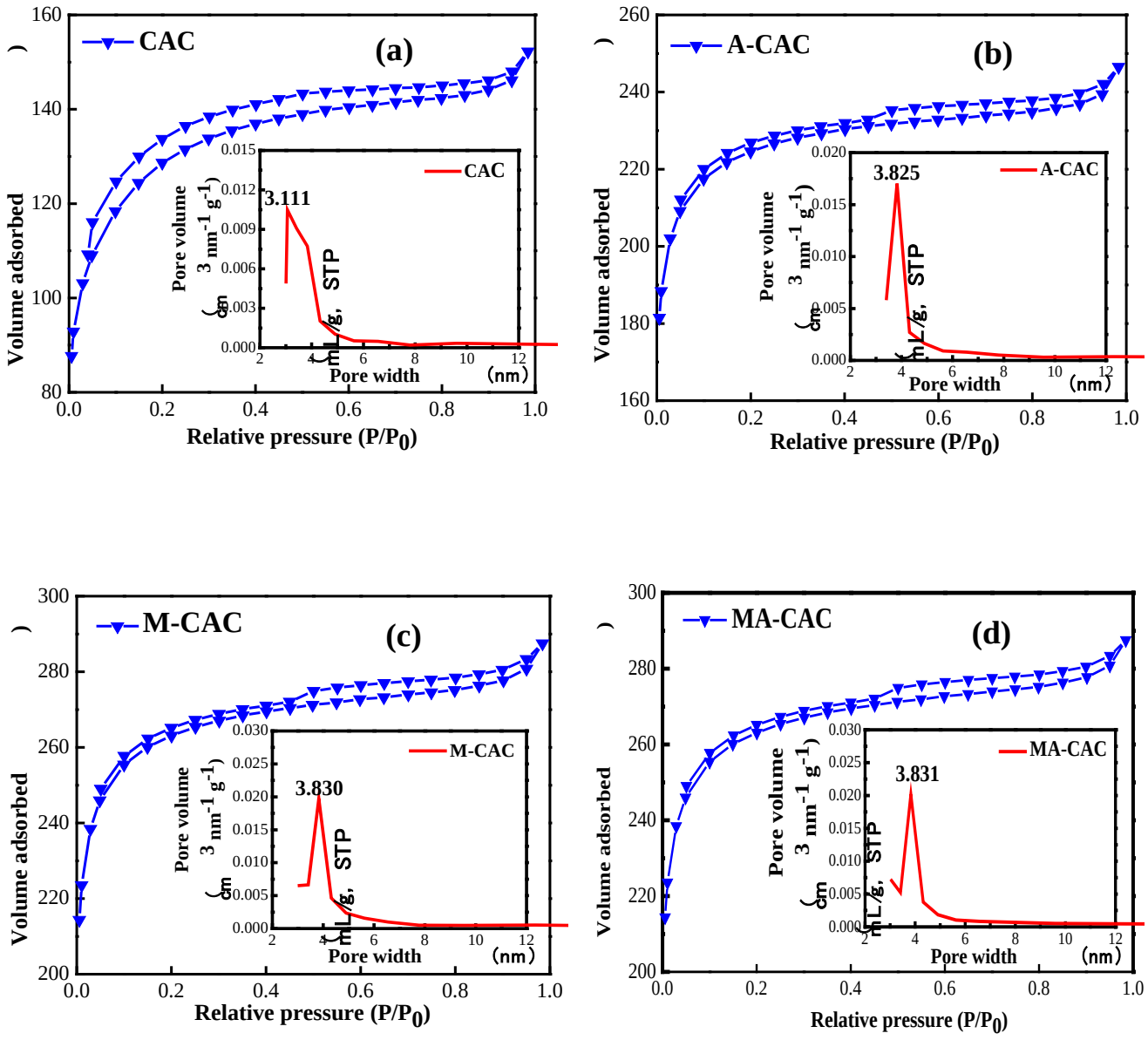

533 **Fig. 2.** Nitrogen adsorption-desorption isotherms and pores size distribution of different activated

534 carbons: (a) CAC; (b) A-CAC; (c) M-CAC; (d) MA-CAC

535

536

537

538

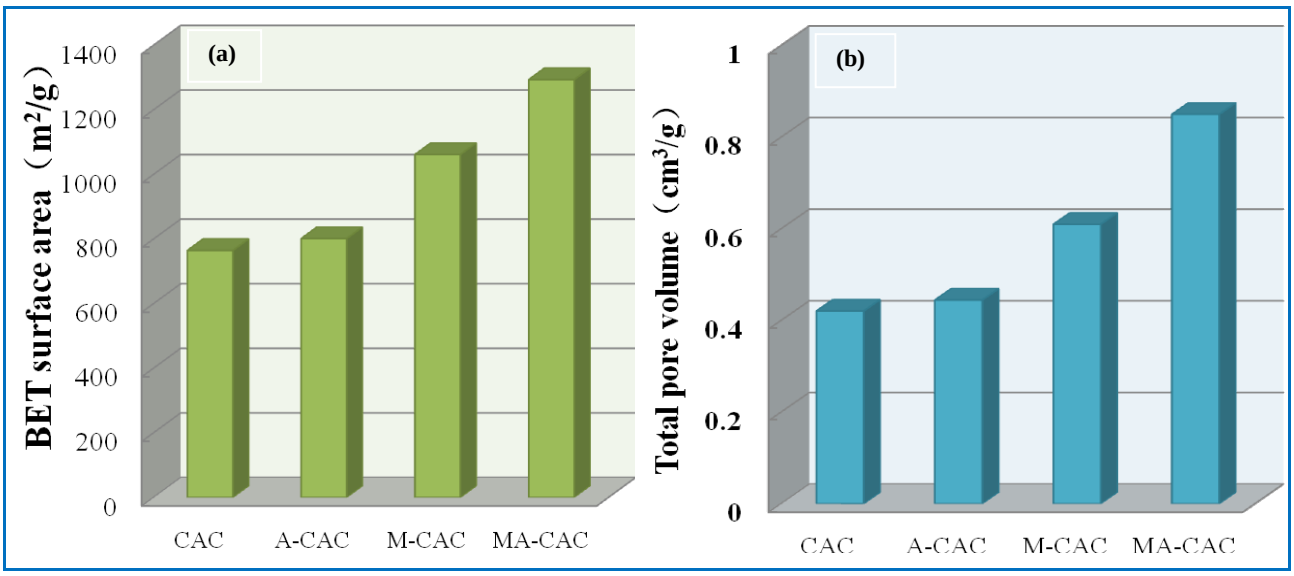

539 **Fig. 3.** Comparison of BET surface area and the porous texture of the CAC and the modified

540 samples (a) BET surface area; (b) Total pore volume

541

542

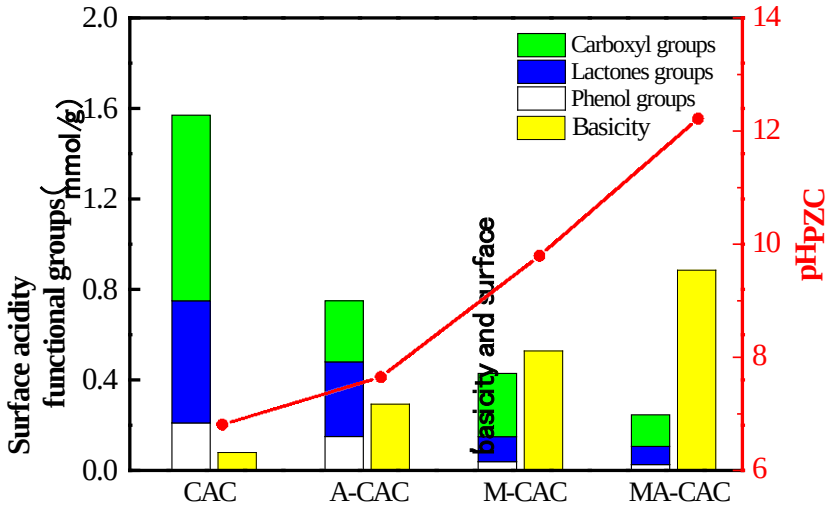

543

544 **Fig. 4.** The surface acidity, basicity, surface functional groups, and pH_{PZC} value of the CAC and the

545 modified samples

546

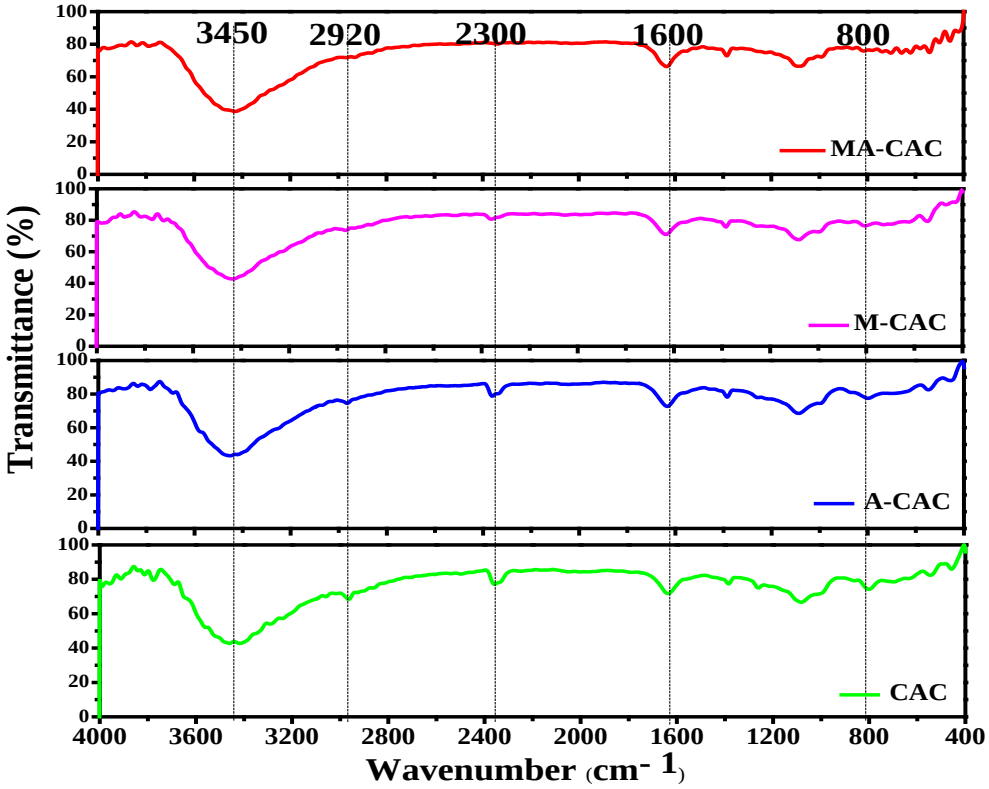

547

548 **Fig. 5.** FTIR spectra of the CAC and the modified samples

549

550

551

552

553

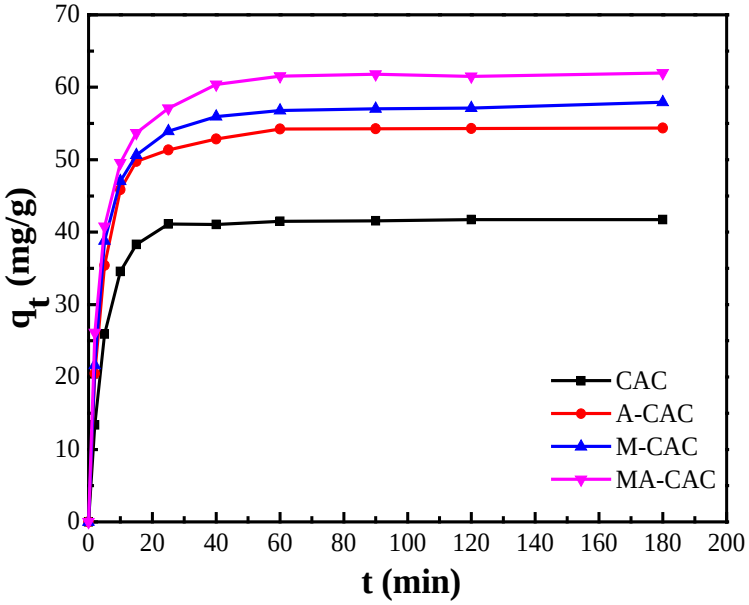

554

555 **Fig. 6.** Adsorbed amount of various carbon materials for pyrene as a function of adsorption time at

556 20 °C (pyrene concentration: 30 mg/L, pyrene solution volume: 100 mL, adsorbents amount: 60

557 mg)

558

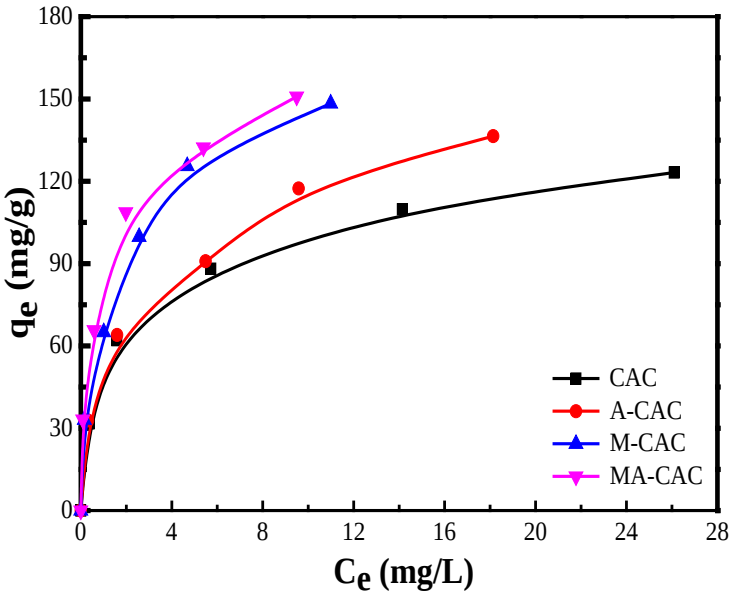

559

560 **Fig. 7.** The adsorbed amount per gram of carbon materials for pyrene as a function of pyrene

561 concentration in solutions at 20 °C (pyrene solution volume: 100 mL, adsorbents amount: 60 mg)

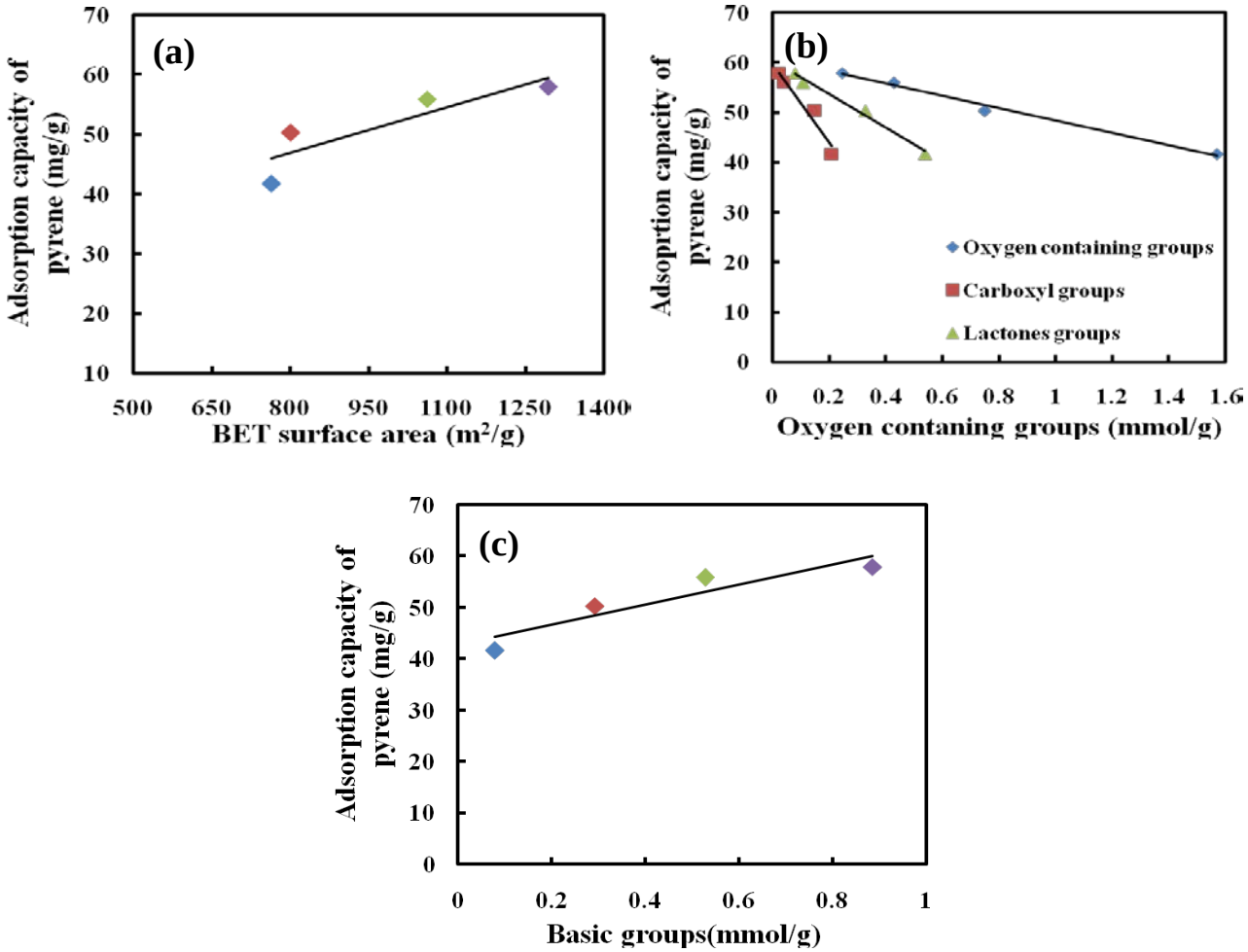

Fig. 8. Adsorption capacity of CAC and the modified samples for pyrene as a function of BET surface area (a); Oxygen-containing groups (b); Basic groups (c)

(Conditions: (a) and (c): ◆ CAC, ◆ A-CAC, ◆ A-CAC, ◆ MA-CAC; (b) in order: CAC, A-CAC, M-CAC, MA-CAC)

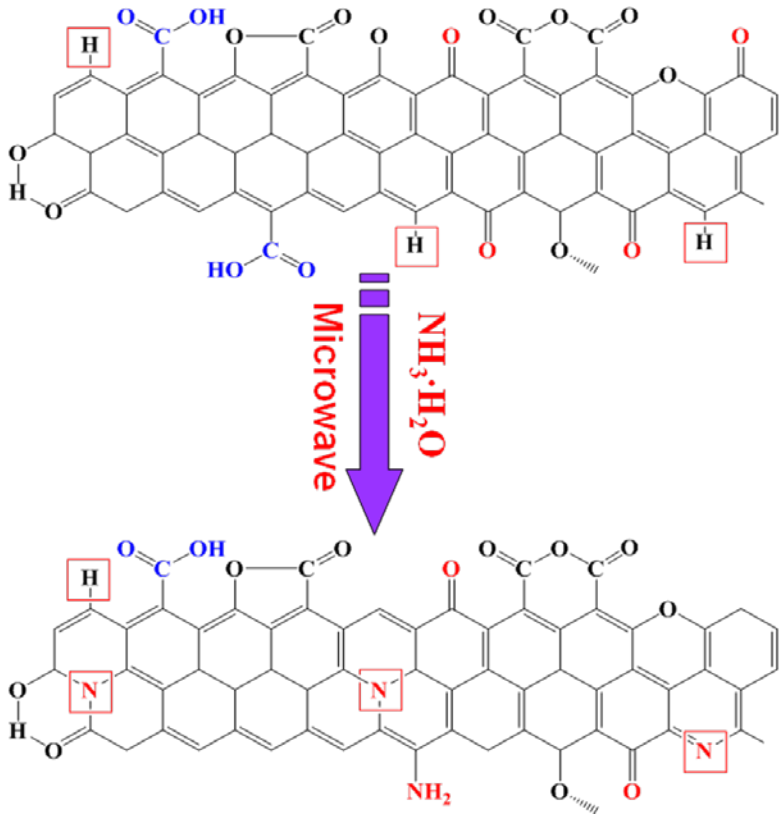

569

570 **Fig . 9.** The change in functional groups of CAC modified to MA-CAC

571

572

573

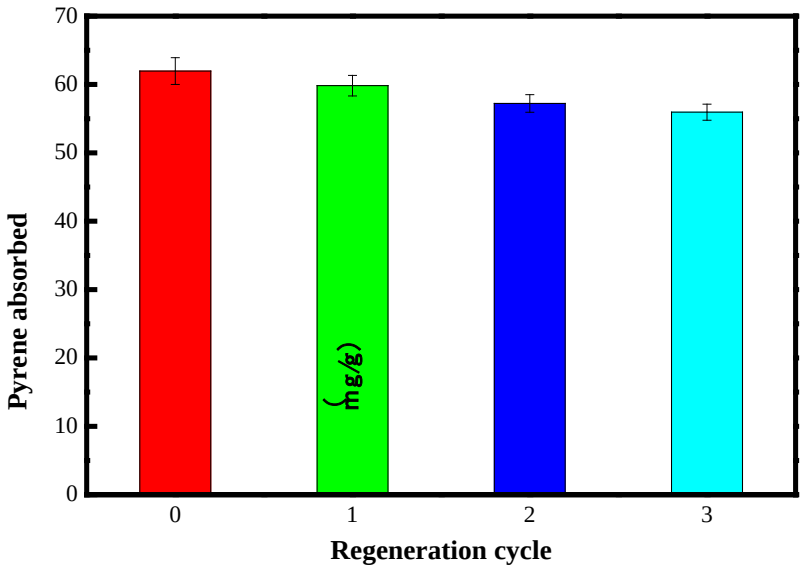

574

575 **Fig. 10.** Adsorption capacities of pyrene onto MA-CAC for three cycles

576

Table 1

Elemental composition of the carbon samples used in the experiment

Samples	Relative content (%)					C/O
	C	H	N	S	O	
Coal	69.75	3.36	0.48	0.45	25.97	2.69
CAC	72.58	1.53	0.51	0.27	25.10	2.89
A-CAC	73.68	1.40	0.73	0.36	23.87	3.09
M-CAC	78.31	1.63	1.59	0.39	18.08	4.33
MA-CAC	82.84	1.11	2.54	0.30	13.20	6.28

Table 2

Parameters of adsorption pseudo-first-order, pseudo-second-order, and intraparticle diffusion kinetic models

Samples	q_{exp}	Pseudo-first-order			Pseudo-second-order			Webber and Morris		Film diffusion	
		$q_{e,cal}$ (mg/g)	k_1 (min^{-1})	R^2	$q_{e,cal}$ (mg/g)	k_2 (g/(mg·min))	R^2	K_p mg/(g·$min^{0.5}$)	R^2	K_{bf} (min^{-1})	R^2
CAC	41.73	36.62	4.58	0.9740	42.63	0.0010	0.9992	0.094	0.2980	0.062	0.8420
A-CAC	54.85	45.00	3.28	0.9900	55.56	0.0013	0.9994	0.430	0.5110	0.052	0.8930
M-CAC	57.93	50.63	3.41	0.8670	58.62	0.0015	0.9996	1.610	0.4810	0.040	0.9380
MA-CAC	61.96	59.97	2.02	0.9340	62.34	0.0019	0.9997	1.440	0.6600	0.025	0.9540

Table 3

Parameters of the isotherms models on the carbon samples

Isotherms models	Parameters	Carbon samples			
		CAC	A-CAC	M-CAC	MA-CAC
Langmuir	q_m(mg/g)	142.86	166.67	200.00	250.00
	K_L(L/mg)	0.47	1.20	0.42	0.44
	R^2	0.9982	0.9620	0.6390	0.9200
Freundlich	K_F	50.60	56.49	66.15	74.66
	1/n	0.3009	0.2370	0.3684	0.3200
	R^2	0.9560	0.9993	0.9991	0.9995

Table 4

Freundlich parameters for adsorption of pyrene obtained by various kinds of adsorbents

Adsorbent	Freundlich		References
	K_F (mg/g)	1/n	
PMO	0.12	1.68	[2]
Chitosan	50.00	0.21	[12]
Rice husk activated carbon	29.71	0.80	[12]
Immature coal	10.00	0.62	[30]
Chitin	120.00	0.14	[33]
MA-CAC	74.66	0.32	This work

599 Table 5 Thermodynamic parameters for adsorption of pyrene onto the CAC and the modified
600 samples

Samples	T (K)	k_2 (g/(mg·min)	K_F	ΔG^o (kJ/mol)	ΔH^o (kJ/mol)	ΔS^o (J/(K· mol))
CAC	283.15	0.0015	51.23	-9.267		
	298.15	0.0010	42.60	-9.144	-11.68	8.56
	313.15	0.0006	36.94	-9.097		
A-CAC	283.15	0.0019	58.08	-9.562		
	298.15	0.0013	45.49	-9.304	-13.47	13.98
	313.15	0.0009	39.85	-9.288		
M-CAC	283.15	0.0023	65.76	-9.854		
	298.15	0.0015	49.87	-9.528	-18.44	30.34
	313.15	0.0012	39.23	-9.248		
MA-CAC	283.15	0.0029	74.25	-10.14		
	298.15	0.0019	53.38	-9.694	-20.64	37.18
	313.15	0.0017	41.66	-9.399		

601

Supplementary material

S.1 X-ray photoelectron spectroscopy (XPS)

The X-ray photoelectron spectra of the CAC and the modified samples were obtained with a model PHI5700 ESCA X-ray photoelectron spectrometer. XPS was applied to determine the surface complexes on the CAC and the modified samples. XPS analysis was conducted using Mg Ka X-ray source (1,253.6 eV) under a vacuum pressure 10^{-6} Pa. The wide scans were conducted from 0 to 1000 eV with a pass energy of 50 eV.

XPS analysis

XPS has been shown to be useful for analyzing the surface chemical characteristics of carbons [19]. Fig. S1 shows the XPS survey spectra of the CAC and the modified samples. The survey spectra of the carbon samples contain distinct peaks for carbon and oxygen. The relationship between the relative peak area and relative content of elements in the carbons is shown in Table 2. The carbon content in modified samples increase, and the oxygen content show the opposite change trend. Meanwhile, the ratio of C/O is rise from 2.41 in CAC surface to 6.22 in the surface of the MA-CAC. Above all, this result still agrees with the results of the element analysis. We can conclude that some oxygen-containing groups are eliminated from the carbons surface. In addition, the result is consistent with the results of surface acidity and basicity.

Table S1 Relative content of various elements on carbon surface in at. %

Carbons	Relative contents (%)				C/O
	C	O	N	S	
CAC	69.97	29.06	0.49	1.48	2.41
A-CAC	75.58	21.68	1.65	1.09	3.49
M-CAC	81.02	16.43	2.25	0.30	4.93
MA-CAC	82.91	13.32	3.55	0.22	6.22

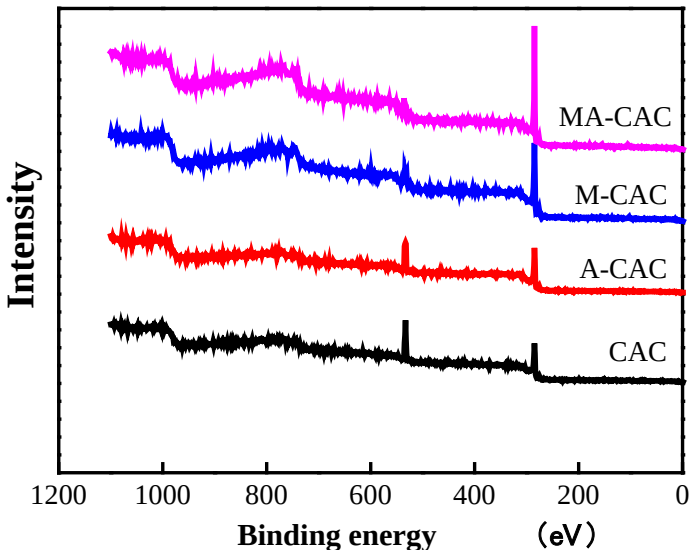

Fig. S1. XPS survey spectra of the CAC and the modified samples

S.2 Effects of ionic strength

Effects of ionic strength to the removal of 100 mL, 30 mg/L pyrene solution by 0.06 g of CAC and the modified samples were studied in the presence of NaCl ions. The concentrations of NaCl were selected as 0.05, 0.10, 0.20, and 0.30 M (mol/L). The mixture was contacted for 60 min. The whole mixture was separated by filtration, and pyrene concentration was measured, then the pyrene adsorption capacity was calculated.

Effect of ionic strength on pyrene adsorption

The results obtained are shown in Fig. S2. It was seen that the adsorption capacity of the pyrene increased in the presence of NaCl. These dissociated Na^+ ions caused a decrease in the adsorption of the pyrene due to electrostatic effects between the carbons and the pyrene molecules [39] (see Fig. S2). The enhanced adsorption capacity of pyrene on CAC and the modified samples also can be explained by the fact that the affinity increased between carbons and pyrene through form a π–π complex between the π-electrons of benzene rings and active sites on the carbons surface [37, 38].

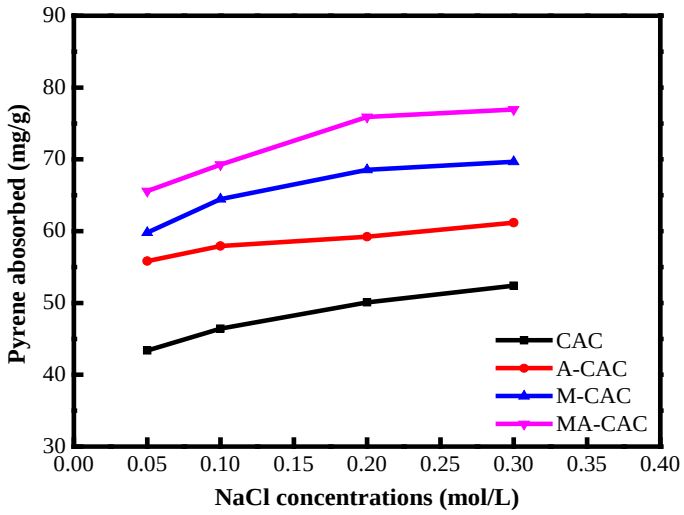

Fig. S2. Effect of ionic strength on pyrene adsorption